Metal–Organic Chemical Vapor Deposition of Copper-Containing Phases: Kinetics and Reaction Mechanisms

Guglielmo G. Condorelli, Graziella Malandrino, and Ignazio Fragalà*

Dipartimento di Scienze Chimiche, Università di Catania, 95125 Catania, Italy

Received May 2, 1994. Revised Manuscript Received July 5, 1994[⊗]

The mechanisms and kinetics of the deposition processes of Cu–O phases by chemical vapor deposition from the $Cu(acac)_2$ precursor were studied under Ar/O_2 in a horizontal flow, low-pressure MOCVD reactor. The nature and the deposition rate of films were determined under different operating conditions (e.g., reactant composition, substrate temperature, and carrier gas flow rate). Fully oxidized CuO films with no carbon contamination were deposited at 723 K and above using $O_2/Cu(acac)_2$ mole ratios $\geq 10^3$. Lower temperatures (in the range 523–723 K) and/or lower $O_2/Cu(acac)_2$ mole ratios (in the range $10–10^3$) gave films of mixed $Cu/Cu_2O/CuO$ composition. The deposition rate under higher temperatures (>593 K) was linearly dependent on the $Cu(acac)_2$ partial pressure. Below this temperature, a saturation limit was approached by increasing the partial pressure. The saturation limit, in turn, was found to increase linearly with the oxygen partial pressure. The dependence of copper deposition rate on the substrate temperature was also investigated and an activation energy value of 48 ± 6 kJ/mol was obtained. The proposed reaction mechanism is based on a dissociative adsorption process of $Cu(acac)_2$ on active surface sites, followed by copper oxidation and ligand decomposition.

Introduction

The metal–organic chemical vapor deposition (MOCVD) of copper films and of other copper-containing phases represent an area of increasing importance to the electronics industry for interconnects between solid state devices.[1,2]

Copper oxide phases produced by MOCVD appear to be of even greater relevance for multicomponent thin films of high-T_c ceramic superconducting materials[3–9] as well as in the fabrication of low cost solar cells.[10–14]

In this context mechanistic aspects involved in the deposition of copper-based phases by MOCVD are of relevance since both the nature and the integrity of phases are crucial for better performing materials. Several MOCVD procedures using various Cu precursors have been reported to date (Table 1).

In this paper we report on low-pressure MOCVD experiments designed to study the kinetics and mecha-

[⊗] Abstract published in *Advance ACS Abstracts,* August 15, 1994.

(1) Pai, P.; Ting, C. H. *IEEE Electron Device Lett.* **1989**, *10*, 423.
(2) Chamberlain, M. B. *Thin Solid Films* **1982**, *91*, 155.
(3) Nakamori, T.; Abe, H.; Kanamori, T.; Shibata, S. *Jpn. J. Appl. Phys.* **1988**, *27*, 1265.
(4) Yamane, H.; Kurosawa, H.; Hirai, T. *Chem. Lett.* **1989**, 939.
(5) Panson, A. J.; Charles, R. G.; Schmidt, D. N.; Szedom, J. R.; Machito, G. J.; Briginski, A. I. *Appl. Phys. Lett.* **1988**, *53*, 1265.
(6) Malandrino, G.; Richeson, D. S.; Marks, T. J.; DeGroot, D. C.; Schindler, J. L.; Kannewurf, C. R. *Appl. Phys. Lett.* **1991**, *58*, 182.
(7) Singh, R.; Sinha, S.; Hsu, N. J.; Chou, P. *J. Appl. Phys.* **1990**, *67*, 1562.
(8) Zhang, K.; Boyd, E. P.; Kwak, B. S.; Wright, A. C.; Erbil, A. *Appl. Phys. Lett.* **1989**, *55*, 1258.
(9) Ciliberto, E.; Fragalà, I. L.; Malandrino, G.; Allen, G. C.; Younes, C. M.; Marks, T. J.; Richeson, D. S.; Schulz, D. L. *Thin Solid Films* **1992**, *216*, 37.
(10) Rakhshani, A. E. *Solid State Electron.* **1986**, *29*, 7.
(11) Rai, B. P. *Sol. Cells* **1988**, *25*, 265.
(12) Olsen, L. C.; Addis, F. W.; Miller, W. *Sol. Cells* **1982–1983**, *7*, 247.
(13) Sears, W. M.; Fortin, E. *Sol. Energy Mater.* **1984**, *10*, 93.
(14) Weichman, F. L.; Reyes, J. M. *Can. J. Phys.* **1980**, *58*, 325.
(15) Gillardeau, J.; Hasson, R.; Oudar, J. *J. Cryst. Growth* **1968**, *2*, 149.
(16) Dejachy, G.; Gillardeau, J.; Rigny, P.; Oudar, J. *Proceedings of the 5th International Conference on Chemical Vapor Deposition*; Blocher, J. M., Hintermann, H. E., Hall, L. H., Eds.; The Electrochemical Society Softbound Proceeding Series: Pennington, NJ, 1975; p 178.
(17) Madar, R.; Bernard, C.; Palleau, J.; Torres, J. *Microelectron. Eng.* **1992**, *19*, 571.
(18) Lampe-Oennerud, C.; Jansson, U.; Haarsta, A.; Carlsson, J. O. *J. Cryst. Growth* **1992**, *121*, 223.
(19) van Hemert, R. L.; Spledlova, L. B.; Sievers, R. E. *J. Electrochem. Soc.* **1965**, *112*, 1123.
(20) Lecohier, B.; Calpini, B.; Philippoz, J. M.; van den Bergh, H.; Laub, D.; Buffat, P. A. *J. Electrochem. Soc.* **1993**, *140*, 789.
(21) Temple, D.; Reisman, A. *J. Electrochem. Soc.* **1989**, *136*, 3525.
(22) Lai, W. G.; Xie, Y.; Griffin, G. L. *J. Electrochem. Soc.* **1991**, *138*, 3499.
(23) Armitage, D. N.; Dunhill, N. I.; West, R. H.; Williams, J. O. *J. Cryst. Growth* **1991**, *108*, 683.
(24) Jeffries, P. M.; Dubois, L. H.; Girolami, G. S. *Chem. Mater.* **1992**, *4*, 1169.
(25) Jain, A.; Chi, K. M.; Kodas, T. T.; Hampden-Smith, M. J.; Farr, J. D.; Paffett, M. F. *Chem. Mater.* **1991**, *3*, 995.
(26) Shin, H. K.; Chi, K. M.; Hampden-Smith, M. J.; Kodas, T. T.; Farr, J. D.; Paffett, M. *Chem. Mater.* **1992**, *4*, 788.
(27) Cohen, S. L.; Liehr, M.; Kasi, S. *Appl. Phys. Lett.* **1992**, *60*, 50.
(28) Kumar, R.; Maverick, A. W. *Chem. Mater.* **1993**, *5*, 251.
(29) Shin, H. K.; Chi, K. M.; Hampden-Smith, M. J.; Kodas, T. T.; Farr, J. D.; Paffett, M. *Adv. Mater.* **1991**, *3*, 246.
(30) Dubois, L. H.; Zegarski, B. R. *J. Electrochem. Soc.* **1992**, *139*, 3295.
(31) Donnelly, V. M.; Gross, M. E. *J. Vac. Sci. Technol., A* **1993**, *11*, 66.
(32) Pauleau, Y.; Fasasi, A. Y. *Chem. Mater.* **1991**, *3*, 45.
(33) Rees, W. S., Jr.; Caballero, C. R. *Adv. Mater. Opt. Electron.* **1992**, *1*, 59.
(34) Rees, W. S., Jr.; Caballero, C. R. *Mater. Res. Soc. Symp. Proc.* **1992**, *250*, 297.
(35) Chang, Y.; Schrader, G. L. *Mater. Res. Soc. Symp. Proc.* **1992**, *250*, 291.
(36) Chichibu, S.; Yoshida, N.; Higuchi, H.; Matsumoto, S. *Jpn. J. Appl. Phys., Part 2* **1992**, *31*, L1778.
(37) Hoke, J. B.; Stern, E. W. *J. Mater. Chem.* **1991**, *1*, 701.
(38) Gerfin, T.; Becht, M.; Dahmen, K. H. *Mater. Sci. Eng., B* **1993**, *B17*, 97.
(39) Marinero, E. E.; Jones, C. R. *J. Chem. Phys.* **1985**, *82*, 1608.
(40) Houle, F. A.; Wilson, R. J.; Baum, T. H. *J. Vac. Sci. Technol., A* **1986**, *4*, 2452.

0897-4756/94/2806-1861$04.50/0

Table 1. Chemical Vapor Deposition (CVD) of Thin Films Containing Copper Phases

CVD method	metal precursor[a]	gas atm	deposited film	ref
conventional	CuF_2 or CuF		copper	15, 16
conventional	$CuCl_2$ or CuCl		copper	17, 18
conventional	$Cu(tfacac)_2$ or $Cu(hfacac)_2$	H_2O/Ar	copper	19
conventional	$Cu(hfacac)_2$	H_2O/He	copper	20
conventional	$Cu(hfacac)_2$	Ar	copper	21
conventional	$Cu(hfacac)_2$	H_2	copper	22
conventional	$Cu(hfacac)_2$	Ar or atm	copper or copper oxide	23
conventional	$Cu(O\text{-}t\text{-}Bu)_4$		copper or copper oxide	24
conventional	(β-diketonate)Cu(alkyne)		copper	25, 26
conventional	(β-diketonate)Cu(COD)		copper	26, 27
conventional	(β-diketonate)Cu(COD)	CO or CO/H_2	copper	28
conventional	(β-diketonate)$CuPR_3$		copper	29, 26
conventional	(hfacac)Cu(vtms)		copper	30, 31
conventional	$Cu(acac)_2$	Ar, H_2, O_2 or H_2O/O_2	copper	32, 33
conventional	$Cu(acac)_2$	N_2, H_2, O_2	copper or copper oxide	34
conventional	$Cu(acac)_2$	O_2	copper oxide	35
conventional	$C_5H_5CuPEt_3$		copper	36
conventional	CuL_2	H_2	copper	37
conventional	Cu(β-ketoiminate)$_2$	H_2	copper or copper oxide	38
laser-assisted	$Cu(hfacac)_2$		copper	39, 40, 41
laser-assisted	$Cu(hfacac)_2Et_x$		amorphous copper-carbon complex	40, 42
laser-assisted	$C_5H_5CuPEt_3$		copper or copper oxide	43
photoassisted	Cu(β-diketonate)$_2$		copper	44
plasma-enhanced	$Cu(hfacac)_2$	H_2O/H_2/Ar or O_2/Ar	copper or copper oxide	45
microwave plasma-enhanced	$Cu(acac)_2$	Ar/H_2	copper	46
microwave plasma-enhanced	$Cu(acac)_2$	Ar, Ar/O_2 or Ar/N_2O	copper or copper oxide	47

[a] tfacac = trifluoroacetylacetonate, hfacac = hexafluoroacetylacetonate, acac = acetylacetonate, O-*t*-Bu = *tert*-butoxide, COD = 1,5-cyclooctadiene, vtms = vinyltrimethylsilane, HL = *N*-(fluoroalkyl)salicylaldimine.

nisms of thin film deposition of Cu−O-based thin films as a function of the most relevant operating variables. The study focuses on the use of the bis(pentane-2,4-dionato)copper(II) coordination complex ($Cu(acac)_2$) as the precursor. This precursor, commonly employed in the thin-film deposition of HT_c superconductors,[6,9] possesses suitable volatility and thermal stability for MOCVD studies. Moreover it has proven a reliable candidate for the production of copper-containing thin films, free from fluorine and nitrogen contamination.

Experimental Section

Experiments were performed in a low-pressure MOCVD reactor made of a silica tube (id = 7.3 cm). The reactor, consisting of some contiguous sections (Figure 1), was evacuated with a double-stage rotary pumping unit. Each section, including the susceptor, was independently heated, with ±2 °C accuracy, using computer-controlled hardware. Films were deposited on glass slides placed on a boron nitride susceptor. The substrates were preliminarily cleaned with a saturated KOH solution, washed with bidistilled water and acetone and, finally, dried in air at 100 °C. The total pressure was held constant in the range 4−5 Torr using a MKS Baratron 122AAX and a vacuum angle valve. Prepurified Ar and O_2 were used as carrier and reaction gases, respectively. The flow rates were controlled using MKS flow controllers and a MKS Multi-gas Controller 147.

Quantitative analyses of Cu (mg/cm^2) in the deposited material were made using a Philips PW 1410/00/60 wavelength-dispersive X-ray fluorescence spectrometer equipped with a tungsten anode and a LiF (220) crystal as secondary radiation

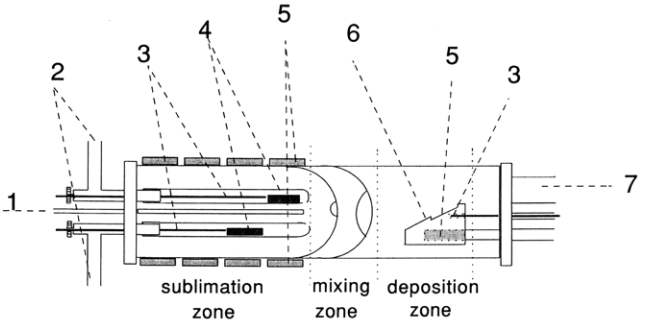

Figure 1. MOCVD reactor. 1 = reaction gas inlet; 2 = carrier gas inlet; 3 = thermocouples; 4 = precursor containers; 5 = heaters; 6 = susceptor; 7 = gas outlet.

dispersive element. The intensities of Cu Kα peaks measured for several Cu and CuO_x MOCVD-deposited standards were used as calibration references. The absolute masses of the above mentioned standards were determined by atomic absorption spectroscopy. X-ray diffraction (XRD) spectra were made using a Philips PW 2103/00 diffractometer equipped with a copper anode. X-ray photoelectron spectra (XPS) were obtained using a PHI 5600 Multy Technique System with a monochromatic Al source. Sputter etching was made with a 2 kV argon ion gun with a beam current of 1 μA. The bis(pentane-2,4-dionato)copper(II) precursor was purchased from Aldrich and was purified by low-pressure sublimation. In all the experiments weighed amounts of the precursor were moved from the cold presublimation section into the preheated sublimation section. The carrier gas was then flowed for different selected times. The total quantity of the sublimed precursor was determined by weight loss measurements. Unless otherwise specified, all experiments were made under steady state conditions at 403 K precursor sublimation temperature (T_{subl}).

Results and Discussion

Influence of the Carrier Gas Flow Rate on the Sublimation of $Cu(acac)_2$. Several experiments were carried out to establish suitable experimental parameters to warrant a local equilibrium regime[21] for precursor sublimation at 403 K. The mass of the $Cu(acac)_2$ sublimed per unit volume of the carrier gas (m/V)

(41) Markwalder, B.; Widmer, M.; Braichotte, D.; van den Bergh, H. *J. Appl. Phys.* **1989**, *65*, 2470.
(42) Wilson, R. J.; Houle, F. A. *Phys. Rev. Lett.* **1985**, *55*, 2184.
(43) Dupuy, C. G.; Beach, D. B.; Hurst, J. E.; Jasinski, J. M. *Chem. Mater.* **1983**, *1*, 16.
(44) Zama, H.; Miyake, T.; Hattori, T.; Oda, S. *Jpn. J. Appl. Phys., Part 2* **1992**, *31*, L588.
(45) Oehr, C.; Suhr, H. *Appl. Phys. A* **1987**, *45*, 151.
(46) Pelletier, J.; Pantel, R.; Oberlin, J. C.; Pauleau, Y.; Gouy-Pailler, P.; *J. Appl. Phys.*, **1992**, *70*, 3862.
(47) Wisniewski, B.; Durand, J.; Cot, L. *J. Phys. IV* **1991**, *1*, C2/389.

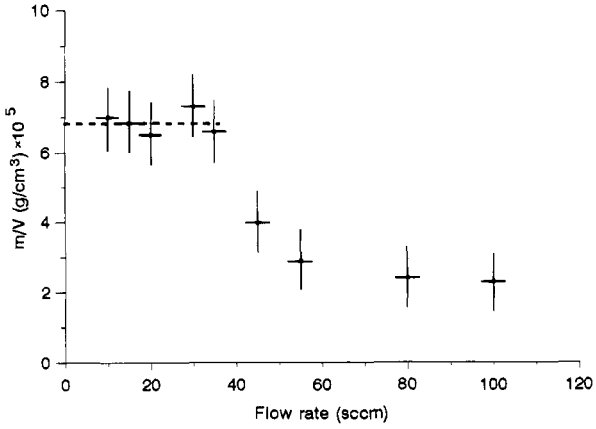

Figure 2. Dependence of the m/V ratio upon the flow rate (F). The dotted line shows the range of flow rates under which sublimation takes place in an equilibrium regime.

depended on the flow rate (F) of the carrier gas itself. The ratio m/V remained constant in the range 0–40 sccm (Figure 2) thus indicating that the sublimation process took place in a quasi-equilibrium regime under these conditions.[21] The same data in Figure 2 were also used to determine the standard sublimation enthalpy of the $Cu(acac)_2$ precursor ($\Delta H°_{298K}$) using the Clausius–Clapeyron equation and assuming an ideal behavior to evaluate the equilibrium vapor pressure of the precursor at 403 K.[21] The required standard entropy, $\Delta S°$, and heat capacity, C_p, values have been taken from ref 48. The 60 ± 2 kJ/mol value obtained here is in good agreement with previously reported values.[32]

Influence of Reactor Operating Variables. Under constant flow rate of reaction (O_2) and carrier (Ar) gases (200 and 30 sccm, respectively) the chemical nature of the deposited films depended on several operating variables, namely the susceptor temperature (hence of the target substrate) and the $O_2/Cu(acac)_2$ mole ratio (R).

Figure 3 shows the X-ray diffraction patterns of films deposited at various susceptor temperatures at a R value of 10^3. Below 573 K, Cu and Cu_2O were present. In the range 573–723 K both Cu_2O and CuO became evident, while above 723 K only CuO was present.

Figure 4 shows the X-ray diffraction patterns of films deposited at susceptor temperature of 723 K and at various values of R.[49] Films were made exclusively of CuO for $R = 10^3$. At $R = 10^2$ CuO and Cu_2O were evident and a mixture of Cu and Cu_2O was present for $R = 10$.

The XPS spectra (Figure 5) provide a clear indication that the deposited films have carbon contamination only on the surface, not in the bulk, since contamination can be easily removed by Ar-sputtering revealing the non-contaminated bulk.

Deposition Rate. The deposition rate of copper was investigated under several operating conditions. In all cases the total pressure inside the reactor was kept constant at 4.3 Torr.

Under the constant flow rates of both the reaction gas (O_2) and the carrier gas (Ar), 200 and 30 sccm, respectively, and under constant $Cu(acac)_2$ partial pressure

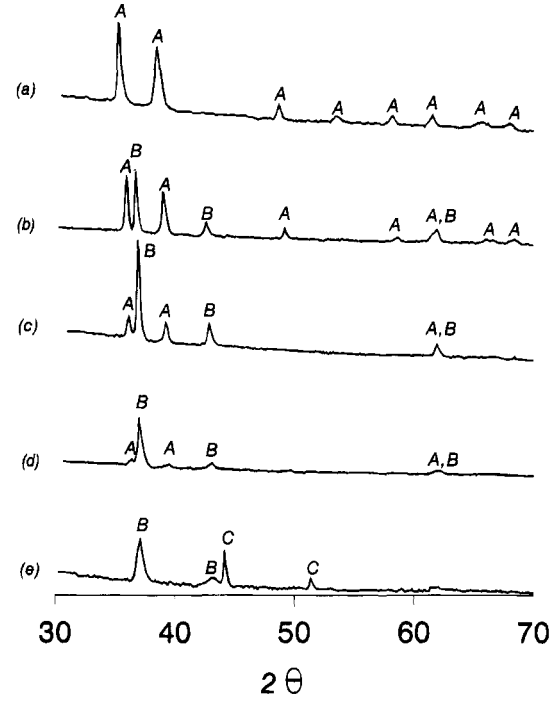

Figure 3. XRD patterns of films deposited at various susceptor temperatures ($R = 10^3$; reaction gas (O_2) flow rate = 200 sccm; carrier gas (Ar) flow rate = 30 sccm): (a) 723 K, (b) 693 K, (c) 663 K, (d) 613 K, (e) 573 K. A = CuO; B = Cu_2O; C = Cu.

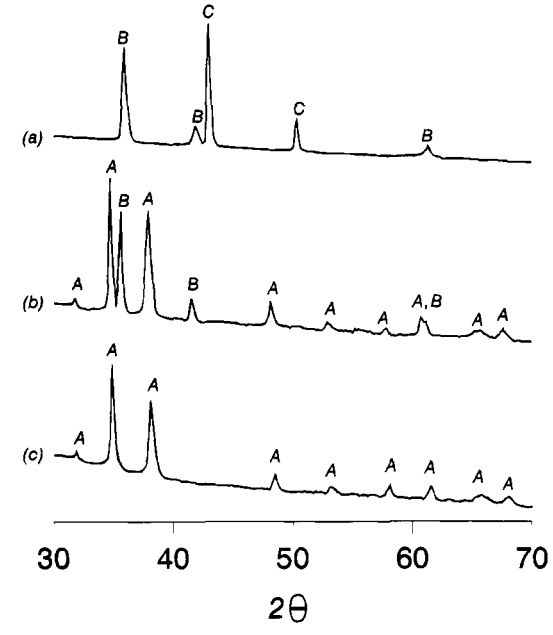

Figure 4. XRD patterns of films deposited under various R = $O_2/Cu(acac)_2$ mole ratios at 723 K susceptor temperature: (a) $R = 10$, (b) $R = 10^2$, (c) $R = 10^3$. A = CuO; B = Cu_2O; C = Cu.

(2.8 × 10^{-3} Torr), the deposition rate of copper-containing films depended on the susceptor temperatures in the range 523–723 K ($R = 1.3 \times 10^3$). The data in Figure 6 show that the deposition process occurred in two different regimes. Below 593 K the process rate is surface-reaction-rate limited since the log of the deposition rate (μg of Cu/cm² min) depended linearly on the reciprocal of the temperature. The activation energy calculated from the Arrhenius plot is 48 ± 6 kJ/mol. Above 593 K, the deposition rate was constant, there-

(48) Teghil, R.; Ferro, D.; Bencivenni, L.; Pelino, M. *Thermochim. Acta* **1981**, *44*, 213.
(49) Different R values have been obtained by varying the sublimation temperatures in the 403–443 K range.

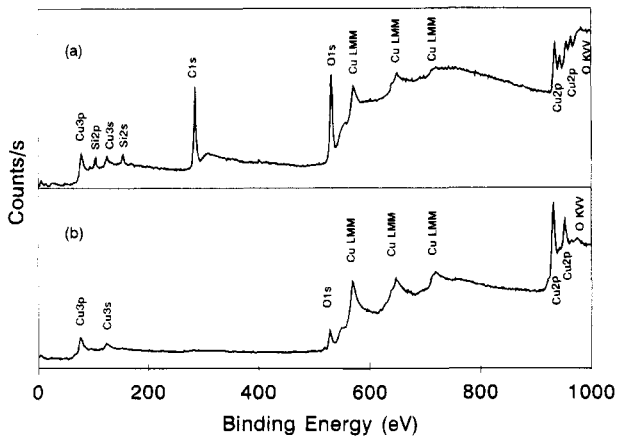

Figure 5. X-ray photoelectron spectra of films deposited using O_2 as reaction gas: (a) as grown, (b) after sputtering (4 min).

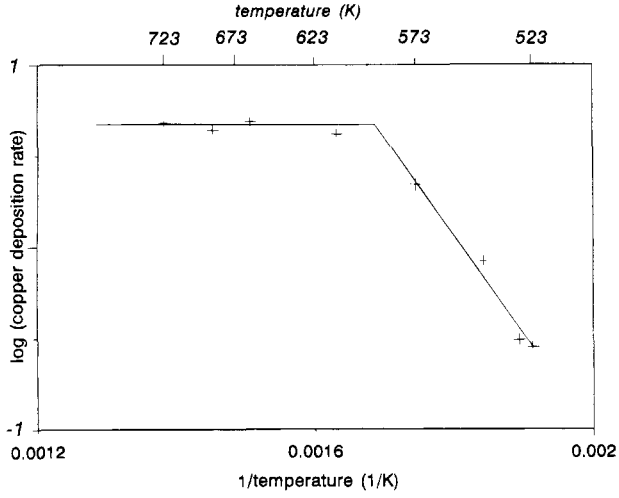

Figure 6. Arrhenius plots of deposition rate (μg/cm^{2}min) vs $1/T$ (1/K).

fore, the process may be feed rate or diffusion rate limited since the precursor is consumed in the surface reaction faster than it can be supplied from the sublimation zone. Experiments carried out in the mass transport limited regime (above 593 K) showed that the deposition rate depended linearly on Cu(acac)$_2$ partial pressure (Figure 7) in the range investigated (1.46×10^{-3}–10.77×10^{-3} Torr).

Above 723 K a growth rate of 0.5 μm/h was calculated at the Cu(acac)$_2$ partial pressure of 2.62×10^{-3} Torr. In these conditions pure CuO films were obtained, and therefore the growth rate can be easily evaluated by using both the X-ray fluorescence analysis to measure CuO surface density (g/cm^2) and literature data[50] for CuO density (g/cm^3).

The dependence of the copper deposition rate on both the Cu(acac)$_2$ partial pressure (9×10^{-5}–9.3×10^{-3} Torr) and the oxygen partial pressure (2.22–3.74 Torr)[51] was thoroughly investigated at 573 K (surface reaction rate limited regime) in order to throw light on the reaction mechanisms.

The deposition rate increased with the Cu(acac)$_2$ partial pressure until a constant saturation limit was

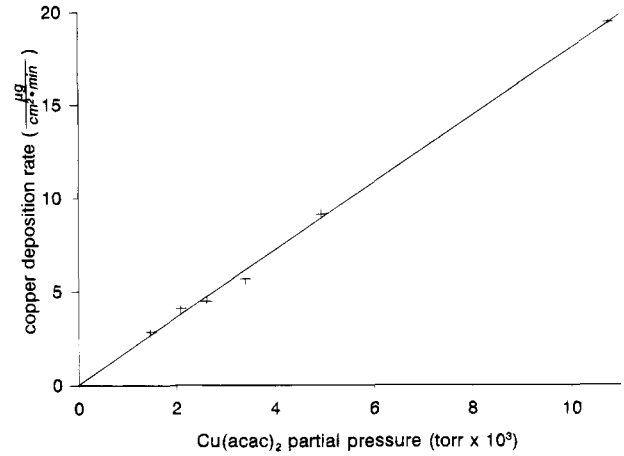

Figure 7. Dependence of the deposition rate upon the Cu(acac)$_2$ partial pressure above 593 K (mass transport limited regime). Reaction gas (O_2) flow rate = 200 sccm; carrier gas (Ar) flow rate = 30 sccm.

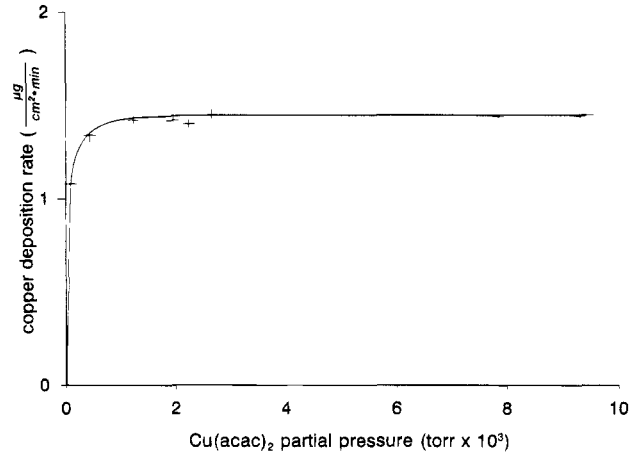

Figure 8. Dependence of deposition rate on Cu(acac)$_2$ partial pressure. T = 573 K; reaction gas (O_2) flow rate = 200 sccm; carrier gas (Ar) flow rate = 30 sccm; P_{tot} = 4.73 Torr; P_{O_2} = 3.74 Torr.

obtained for partial pressures higher than 15.3×10^{-3} Torr (Figure 8). In this saturation range the reaction is zero order with respect to Cu(acac)$_2$. This behavior indicates that the rate-limiting step involves a surface reaction where the active sites become saturated under high Cu(acac)$_2$ partial pressure. In addition, it was found that the saturation limit value depended linearly on oxygen partial pressure (Figure 9) thus implying that the reaction is first order with respect to the oxygen partial pressure.

Reaction Mechanism. Previous mechanistic studies of copper deposition suggest that the metal–ligand bond is easily broken on surface active sites.

Girolami et al.,[52] who studied Cu(acac)$_2$, Cu(hfacac)$_2$, and Cu(hfacac)(vtm) adsorption processes by vibrational and mass spectroscopies, have reported that these molecules adsorb dissociatively on the surface thus forming copper and adsorbed ligands. The ligands (Figure 10a) are oriented perpendicular to the surface and are bonded to active sites by the carbonyl oxygen atoms.

In contrast, on the basis of XPS and HREELS experiments, Cohen et al.[27] suggested that Cu(hfacac)$_2$ adsorbs

(50) *CRC Handbook of Chemistry and Physics*, 65th ed.; Weast, R. C., Astle, M. J., Beyer, W. H., Eds.; CRC Press, Inc.: Boca Raton, FL, 1984.

(51) Different oxygen partial pressures have been obtained by varying O_2/Ar flow rate ratio in the reaction gas.

(52) Girolami, G. S.; Jeffries, P. M.; Dubois, L. H. *J. Am. Chem. Soc.* **1993**, *115*, 1015.

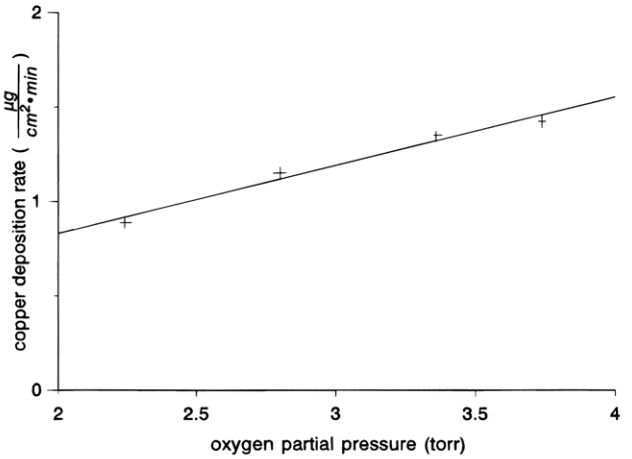

Figure 9. Dependence of deposition rate on oxygen partial pressure. Reaction gas (Ar/O_2) flow rate = 200 sccm; carrier gas (Ar) flow rate = 30 sccm; $T = 573$ K; $P_{tot} = 4.3$ Torr; $P_{Cu(acac)_2} = 9.3 \times 10^{-3}$ Torr.

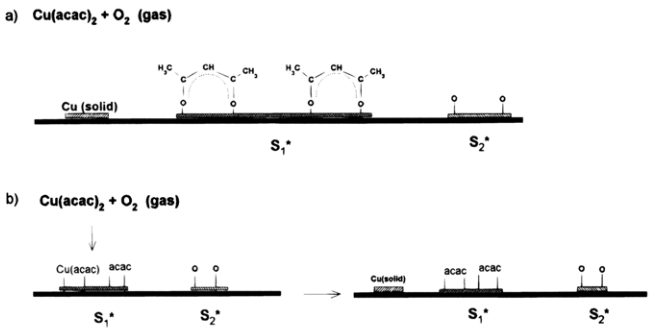

Figure 10. Proposed mechanisms for MOCVD experiments.

dissociatively thus giving Cu(hfacac) and hfacac (Figure 10b).

Rees et al.[34] suggested that in Cu_2O deposition, copper is first deposited as Cu^0 and, then, oxidized to Cu_2O.

Differential scanning calorimetry experiments on $Cu(acac)_2$ (Chang et al.[35]) indicated two different steps for the metal−ligand dissociation and the reaction between O_2 and the ligand.

In this perspective, the present experimental results become consistent with the following reaction scheme (Figure 10) in which $Cu(acac)_2$ adsorbs dissociatively on active surface sites (S_1*) in one [1] or more steps [1a] and [1b]. The adsorption of $Cu(acac)_2$ is irreversible, with the Cu atoms becoming part of the film surface.

Reversible dissociative adsorption on different surface sites S_2* occurs for O_2 [2]. Note that two different active sites S_1* and S_2* must be assumed in the process, as a consequence of the already discussed linear dependence of the deposition rate on the O_2 partial pressure when the active sites for $Cu(acac)_2$ adsorption are already saturated. In addition, the assumption that the same active sites are involved for both $Cu(acac)_2$ and O_2 adsorption gives deposition rate expressions which do not agree with the present experimental results.

$$Cu(acac)_2\,(g) + S_1^* \xrightarrow{k_1} Cu(s) + 2acac(ad) \quad [1]$$

or

$$Cu(acac)_2\,(g) + S_1^* \rightarrow Cu(acac)(ad) + acac(ad) \quad [1a]$$

$$Cu(acac)(ad) \rightarrow Cu(s) + acac(ad) \quad [1b]$$

$$O_2\,(g) + S_2^* \overset{K}{\rightleftharpoons} 2O\,(ad) \quad [2]$$

Adsorbed acac ligands undergo decomposition into volatile byproducts when reacting with adsorbed O atoms [3].

$$2acac(ad) + 2O\,(ad) \xrightarrow{k_3} \text{volatile byproducts} + S_2^* + S_1^* \quad [3]$$

The deposited copper is oxidized by adsorbed O atoms [4] and [5].

$$4Cu(s) + 2O\,(ad) \rightarrow 2Cu_2O(s) + S_2^* \quad [4]$$

$$2Cu_2O(s) + 2O(ad) \rightarrow 4CuO(s) + S_2^* \quad [5]$$

The regeneration of active sites by acac decomposition in step [3] represents the rate-limiting step of the overall reaction.

The deposition rate (r_1) is

$$r_1 = k_1 P_{Cu(acac)_2} \theta_1 \quad (1)$$

where θ_1 is the fraction of unoccupied active sites S_1*.

From steps [2] and [3] and assuming that the fraction of active sites S_2* occupied by adsorbed oxygen atoms is negligible in equilibrium conditions, the rate (r') of ligand decomposition is

$$r' = k' P_{O_2} (1 - \theta_1) \quad (2)$$

where $k' = Kk_3$ and $(1 - \theta_1)$, equal to [2acac(ad)], represent the fraction of active sites occupied by adsorbed ligands.

In the steady-state conditions, the fraction of unoccupied active sites remains constant, and therefore

$$r_1 = r' \quad (3)$$

From eqs 1−3 the deposition rate is

$$r_1 = \frac{k_1 k' P_{O_2} P_{Cu(acac)_2}}{k_1 P_{Cu(acac)_2} + k' P_{O_2}} \quad (4)$$

The same expression can be arrived at by assuming steps [1a] and [1b] instead of [1] under steady-state conditions. Therefore, there is no experimental evidence of whether [1] or [1a] and [1b] mechanisms apply to the present experiments.

Equation 4 fits well the experimental results in Figures 8 and 9. In fact, at high $Cu(acac)_2$ partial pressure ($k_1 P_{Cu(acac)_2} \gg k' P_{O_2}$), eq 4 becomes

$$r_1 = k' P_{O_2} \quad (5)$$

Thus, the deposition rate becomes zero order with respect to $P_{Cu(acac)_2}$ (Figure 8) and first order with respect to P_{O_2} (Figure 9).

Additonal support for the proposed deposition mechanism become evident when considering the general expression (4) of the deposition rate in the reciprocal form:

$$\frac{1}{r_1} = \frac{1}{k'P_{O_2}} + \frac{1}{k_1 P_{Cu(acac)_2}} \quad (6)$$

Plots (Figure 11) of $1/r_1$ vs both $1/P_{Cu(acac)_2}$ (under constant P_{O_2}) and $1/P_{O_2}$ (under constant $P_{Cu(acac)_2}$ give good straight lines. Moreover, the values of k' obtained from the two sets of independent data are almost identical within experimental error. A similar agreement is found as far as k_1 is concerned. Note, however, that data in Figure 11 only provide the lower limit of the k_1 since they are related to experiments made under saturation conditions ($k_1 P_{Cu(acac)_2} \gg k'P_{O_2}$).

In this context the proposed mechanism, which assumes consecutive steps for the deposition and oxidation process of copper, is tuned well with the observed dependence of the copper oxidation state upon both the temperature and the $O_2/Cu(acac)_2$ mole ratio. In fact, higher oxidation states were observed when increasing both the temperature and the $O_2/Cu(acac)_2$ mole ratio thus indicating that the layer by layer oxidation increases faster than the growth of the Cu phase.

Conclusions

The formation of Cu−O phases has been the object of several studies in terms of the preparative and phenomenological implications. There is, by contrast, a paucity of data as far as the mechanistic aspects are concerned. Models to describe MOCVD reactions involved in the deposition of Cu^0 films are well-known, but no fully comprehensive models have been proposed to describe the copper oxide deposition process. The present study provides the first ever model to explain the intriguing role of the O_2 reaction gas in the MOCVD formation of copper oxide films. In addition, this proposed model accounts well for both the kinetic data and the chemical nature of the films.

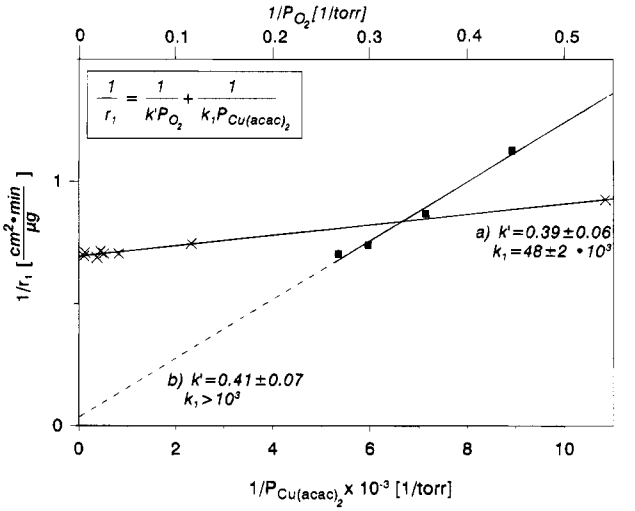

Figure 11. (a) Dependence of $1/r'$ on $1/P_{Cu(acac)_2}$. (×) $[k'] = [k_1] = \mu g\ cm^{-2}\ min^{-1}\ Torr^{-1}$; $P_{O_2} = 3.74$ Torr; $T = 573$ K; reaction gas (O_2) flow rate = 200 sccm; carrier gas (Ar) flow rate = 30 sccm; $P_{tot} = 4.3$ Torr. (b) Dependence of $1/r'$ on $1/P_{O_2}$ (■) $[k'] = [k_1] = \mu g\ cm^{-2}\ min^{-1}\ Torr^{-1}$; $P_{Cu(acac)_2} = 9.3 \times 10^{-3}$; $T = 573$ K; reaction gas (Ar/O_2) flow rate = 200 sccm; carrier gas (Ar) flow rate = 30 sccm; $P_{tot} = 4.3$ Torr.

Finally we note that the present results are of relevance to the design of better performing MOCVD in situ synthetic procedures of HT_c ceramic superconductors. Of course, further work is required to study possible interferences among the components of mixed-oxide matrices.

Acknowledgment. The authors gratefully thank the Consiglio Nazionale delle Ricerche (C.N.R., Rome, Progetto Nazionale Materiali Avanzati) for financial support.